Published in final edited form as:
Stem Cells. 2013 February ; 31(2): 349–359. doi:10.1002/stem.1283.

Ephrin-A3 Suppresses Wnt Signaling to Control Retinal Stem Cell Potency

Yuan Fang[a,b,*], **Kin-Sang Cho**[b,*], **Kissaou Tchedre**[b], **Seung Woo Lee**[c,d], **Chenying Guo**[b], **Hikaru Kinouchi**[b], **Shelley Fried**[c,d], **Xinghuai Sun**[a], and **Dong Feng Chen**[b,c]

[a]Department of Ophthalmology and Visual Science, Eye & ENT Hospital, Shanghai Medical College, Fudan University, Shanghai, P. R. China, 200031

[b]Schepens Eye Research Institute, Massachusetts Eye and Ear, Department of Ophthalmology, Harvard Medical School, 20 Staniford St., MA, 02114

[c] Boston VA Healthcare System, 150 S. Huntington Ave, Boston, MA

[d]Department of Neurosurgery, Massachusetts General Hospital, Harvard Medical School, 185 Cambridge, Boston, MA

Abstract

The ciliary epithelium (CE) of adult mammals has been reported to provide a source of retinal stem cells (RSCs) that can give rise to all retinal cell types *in vitro*. A recent study, however, suggests that CE-derived cells possess properties of pigmented ciliary epithelial cells and display little neurogenic potential. Here we show that the neurogenic potential of CE-derived cells is negatively regulated by ephrin-A3, which is upregulated in the CE of postnatal mice and presents a strong prohibitory niche for adult RSCs. Addition of ephrin-A3 inhibits proliferation of CE-derived RSCs and increases pigment epithelial cell fate. In contrast, absence of ephrin-A3 promotes proliferation and increases expression of neural progenitor cell markers and photoreceptor progeny. The negative effects of ephrin-A3 on CE-derived RSCs are mediated through activation of an EphA4 receptor and suppression of Wnt3a/β-catenin signaling. Together, our data suggest that CE-derived RSCs contain the intrinsic machinery to generate photoreceptors and other retinal neurons, while the CE of adult mice expresses negative regulators that prohibit the proliferation and neural differentiation of RSCs. Manipulating ephrin and Wnt/β-catenin signaling may, thus, represents a viable approach to activating the endogenous neurogenic potential of CE-derived RSCs for treating photoreceptor damage and retinal degenerative disorders.

Corresponding author: Dong Feng Chen, Schepens Eye Research Institute, 20 Staniford Street, Boston, MA 02114 Phone: (617) 912-7490, Fax: (617) 912-0101, dongfeng.chen@schepens.harvard.edu..
*These authors contributing equally to this work.

Author Contributions:
Yuan Fang: data collection, analysis and interpretation, manuscript writing
Kin-sang Cho: data collection, analysis and interpretation, revising the manuscript
Kissaou Tchedre: data collection and analysis
Seung Woo Lee: electrophysiology experimental design, data collection, analysis and interpretation, manuscript writing
Chenying Guo: data collection, analysis and interpretation
Hikaru Kinouchi: data collection, analysis and interpretation
Shelley Fried: electrophysiology experimental design, data analysis and interpretation, manuscript writing, financial support
Xinghuai Sun: Financial support, administrative support, manuscript writing
Dong Feng Chen: Conception and design, financial support, data analysis and interpretation, manuscript writing and revision, and final approval of manuscript

Keywords

Adult stem cells; cell signaling; neural differentiation; retina; stem cell plasticity

INTRODUCTION

Retinal degenerative diseases characterized by death of photoreceptor cells, including age-related macular degeneration, retinitis pigmentosa, and cone dystrophy, are leading causes of irreversible blindness. Photoreceptor cells, like most neurons in the mammalian central nervous system, do not spontaneously regenerate once lost [1]. Stem cell therapy, thus, holds great promise for reversing vision loss and treating these disorders. To date, efforts have been made to identify an endogenous source of retinal stem cells (RSCs) of adult mammals, and cells derived from the ciliary epithelium (CE) of the eye are thought to contain such a group of cells [2].

The ciliary marginal zone (CMZ) of lower vertebrates, such as teleosts and amphibians, is known to harbor a pool of RSCs capable of generating new retinal neurons throughout life [3]. The regenerative process usually starts with the dedifferentiation of pigmented cells; they then proceed to depigmentation, reentrance into the cell cycle and expression of neural retinal progenitor genes [4, 5]. Although the retinas of adult mammals do not regenerate, a population of multipotent RSCs has been isolated from the CE of adult rodents and humans that can give rise to all retinal cell types *in vitro* [2, 6-8]. However, their ability to proliferate and generate new retinal neurons, such as photoreceptors, appears to be limited *in vivo* [9-11]. Mitogens, including basic fibroblast growth factor (bFGF), insulin, Wnt3a, and pigment epithelium-derived factor, are found to promote the proliferative potential of CE-derived RSCs [12-16]. Transcription factors, such as OTX2, Crx and Chx10, increase the photoreceptor progeny of CE-derived RSCs [17]. Recent reports, however, suggest that the CE-derived cells of adult mammals possess pigmented ciliary epithelial cell properties and are incapable of differentiating into retinal neurons or photoreceptors [10, 11]. This study argues against the validity of the existing theory that CE-derived cells present an endogenous source of RSCs for cell replacement therapy to treat retinal neurodegeneration without prerequisite reprogramming.

We have previously reported that the neurogenic potential of central nervous system (CNS) stem cells is critically regulated by positional cues in the local environment and is prohibited by expression of high levels of growth inhibitors, such as ephrin-A2 and -A3, in adult mice [18]. Ephrins and Eph receptors are pivotal regulators of pattern formation, cell migration, axonal guidance, and synaptogenesis during CNS development [19]. Accumulating evidence indicates that ephrin-As, acting through receptor EphA7, negatively regulate neural stem cell survival and proliferation in the developing telencephalon [20] and subventricular zone [21], or in the non-neurogenic CNS regions of adult mice [18, 22]. Absence of ephrin-A2 and -A3 in adult mice results in active ongoing neurogenesis in diverse CNS regions [18]. These findings led to our hypothesis that ephrins also participate in the control of the neurogenic program of CE-derived cells in adult mice by functioning as a negative regulator. To address this hypothesis, we set out to test whether ephrin-As suppress the neurogenic potential of CE-derived cells and whether manipulating ephrin signaling is sufficient to promote the neurogenic program and photoreceptor potential of these RSCs.

MATERIALS AND METHODS

Animals

Ephrin-A3$^{-/-}$ mice were generated as previously described [18], and C57BL/6J wild-type mice were purchased from Charles River Laboratories (Wilmington, MA). Mice older than 2 months were referred to as adult. All experimental procedures and use and care of animals followed a protocol approved by the Animal Care and Use Committee at the Schepens Eye Research Institute, Harvard Medical School.

Preparation of CE-derived Cell and Neurosphere Cultures

As previously described [2], briefly, mouse eyeballs were hemisected; the CE was carefully dissected free from all surrounding tissues and dissociated using a papain-based dissociation system (Worthington Biochemical; Lakewood, NJ) according to the manufacturer's instructions. Dissociated cells were resuspended in Dulbecco's Modified Eagle's medium (DMEM)/Ham's F-12 medium (F12) (1:1; Invitrogen; Carlsbad, CA, http://www.invitrogen.com) containing N2 supplement (1:100; Invitrogen), epidermal growth factor (EGF) (20 ng/ml; Sigma-Aldrich), basic fibroblast growth factor (20 ng/ml; Sigma-Aldrich), heparin (2 μg/ml; Sigma-Aldrich) and 1% penicillin-streptomycin (Sigma-Aldrich). Cells were plated at a density of 2×10^4 cells per well in a 24-well culture plate. Fresh growth factors were added every other day, and the medium was changed every 5-7 days. Neurospheres (NSs), which were defined as free-floating spheres with a defined outer boundary and a diameter >40 μm, were counted after 7 days of incubation [6]. A minimum of 5 wells were counted per group, and each experiment was repeated at least 3 times. For self-renewal studies, individual NSs were collected, dissociated and seeded at a clonal density of 2×10^4 cells per well in a 24-well plate. After 14 days of incubation, secondary NSs were counted [8, 23].

Cell Proliferation Assay

To study cell proliferation, primary NS obtained after 7 days in culture were dissociated to a single cell suspension and seeded in 96-well culture plates at a density of 1,000 cells per well, in DMEM/F12 medium containing 10% fetal bovine serum (FBS; Invitrogen) for 48 hours. 5-bromo-2-deoxyuridine (BrdU; 0.5 μM; Sigma-Aldrich) was added to the culture media 4 hours before fixation. Cell nuclei were stained with the nuclear marker 4 ,6-diamidino-2-phenylindole dihydrochloride (DAPI; Vector Laboratories, Burlingame, CA) and counted, and the percentage of BrdU+ cells was recorded. The results presented were obtained from a minimum of 3 independent experiments. To investigate the effect of ephrin-A3 on the proliferation and didderentiation of CE-derived cells *in vitro*, antibody-clustered ephrin-A3 (300 ng/ml; R&D systems; Minneapolis, MN) or control Fc (300 ng/ml; R&D Systems) were added to dissociated NS cell cultures. Antibody-clustered forms of proteins were generated by incubating the protein with anti-human IgG (Jackson Immuno Research Laboratories; West Grove, PA) for 1 hour at room temperature before application [18, 21]. In some experiments, recombinant mouse Wnt3a (20 – 50 ng/ml; R&D Systems) were added to the culture medium. To investigate the role of EphA4 receptor in the proliferation of CE-derived RSCs, the EphA4 soluable protein (2.5 μg/ml; R&D Systems) or control Fc (2.5 μg/ml) were added to the culture medium.

Cell Differentiation Assay

To study the differentiation potential of CE-derived RSCs, 7-day-old CE-derived NSs were dissociated in a 0.25% Trypsin-EDTA (Sigma) solution. Cells were plated at a density of 1×10^4 cells per well in a 24-well plate pre-coated with Poly-L-Ornithine (10 μg/ml) and laminin (100 ng/ml, both from Sigma-Aldrich). The cultures were maintained in Neurobasal

medium (Invitrogen) containing B27 supplement (Invitrogen), penicillin/streptomycin, 2 mM L-glutamine (Invitrogen), and 1% FBS for 10-21 days, and the medium was changed every 3-4 days.

Immunofluorescence Staining

Immunofluorescence staining was performed using a standard protocol. Primary antibodies used included rat anti-BrdU (1:100; Abcam; Cambridge, MA), mouse monoclonal antibodies specific for ß-III-tubulin (Tuj1; 1:200; BD Biosciences; San Jose, CA) and microtubule-associated protein 2 (MAP2; 1:100; Santa Cruz Biotechnology; Santa Cruz, CA), rabbit anti-recoverin antibody (1:1000; Chemicon; Bellerica, MA), sheep anti-Chx10 antibody (1:500, Abcam), rabbit anti-glial fibrillary acidic protein (GFAP) antibody (1:1000; Sigma-Aldrich), rabbit anti-ephrin-A3 antibody (1:100; Santa Cruz Biotechnology), rabbit anti-EphA4 antibody (1:100; Abcam), and secondary antibodies conjugated with Cy2, or Cy3 (Jackson Immunoresearch Laboratories). The slides were mounted with VECTASHIELD mounting media (H-1200; Vector Labs; Burlingame, CA).

Quantification of Cell Proliferation *in vivo*

To label proliferating cells *in vivo*, adult C57BL/6J wild-type and ephrin-A3$^{-/-}$ mice received intraperitoneal injections (twice daily) of BrdU (50 mg/kg; Sigma-Aldrich) dissolved in 0.9% sterile saline for 7 consecutive days. Seven days after the first BrdU injection, mice were killed and transcardially perfused with 4% paraformaldehyde (Sigma-Aldrich). Transverse cryosections of the mouse eyes (12 μm) were pre-treated with HCl (2.0 N; Sigma-Aldrich) for 1 hour at 37°C and subjected to BrdU immunolabeling. Eyeball sections were counterstained with DAPI (1 mg/ml) in phosphate buffered saline (PBS; Sigma-Aldrich) to reveal cell lamina structures. Cells stained positive for BrdU were counted, and a minimum of 20 sections per mouse, 9 mice per group, were analyzed.

Reverse Transcription-Polymerase Chain Reaction (RT-PCR) and Real-time PCR

Total RNAs were extracted from 7-day-old CE-derived primary NS or from NS-derived cells at 10 days after induction of differentiation, using TRIzol reagent (Invitrogen) in accordance with the manufacturer's instructions. Reverse transcription was performed using TaqMan RT reagents (P/N N808-0234; Applied Biosystems; Carlsbad, CA). Quantitative detection of specific mRNA transcripts was carried out by real-time RT-PCR using an ABI7900 HT Sequence Detection System (Applied Biosystems). Primers were designed using OligoPerfect™ Designer software provided on the Invitrogen website (http://tools.invitrogen.com/content.cfm?pageid=9716) or as previously described [10]. The sequences of all primers are listed in Supplemental Table 1. Samples were analyzed in triplicate, and relative amounts of mRNAs determined by normalizing to β-actin and Glyceraldehyde 3-phosphate dehydrogenase (GADPH) expression levels. The same primers were used for conventional RT-PCR, which was carried out at a 60°C annealing temperature for 32 cycles.

Immunoprecipitation and Immunoblotting

Tissues or cultured stem cells were lysed with lysis buffer (100 mM HEPES/KOH, 1 mM EDTA, 200 mM KCl, 20% glycerol, 0.1% IGEPAL, 1 mM DTT, 0.1 mM PSMF, 0.2 mM sodium orthovanadate) and subjected to centrifugation at 12,000 rpm for 10 minutes. Co-immunoprecipitation assays were performed using Protein G Magnetic Beads, following the manufacturer's protocol (S1430S, New England Biolabs Inc.; Ipswich, MA). Cell or retinal tissue lysates (20-50 μg per lane) were loaded onto 4-20% Precise Protein Gels (Thermo Scientific; Rockford, IL) followed by Western blotting with an anti-mouse phosphotyrosine antibody (4G10; 1:1000, Millipore; Upstate, NY), rabbit anti-EphA4 (1:100; Abcam), rat

anti-EphA7 (1:100; Abcam), rabbit anti-ephrin-A3 (1:100; Santa Cruz Biotechnology), rabbit anti-β-catenin (1:4000; Abcam). Mouse monoclonal β-actin antibody (1:5000; Abcam) or mouse monoclonal GAPDH antibody conjugated to Chemiluminescent horseradish peroxidase (HRP) Substrate (1:5000; Abcam) was used as loading controls. Membranes were incubated with appropriate horseradish peroxidase-conjugated secondary antibodies (1:5000-1:10000; GE Healthcare UK, Ltd.) and analyzed quantitatively using ImageJ software (NIH, Bethesda, MD). Quantitative data were presented as mean ± S.D. from triplicate experiments.

Electrophysiology

CE-derived RSCs were induced to differentiate as describe above. At 1, 3 and 5 weeks post differentiation, cells with round somas and neurites were selected for electrophysiological recording. Spiking was recorded with a patch electrode (4-8 MΩ, filled with Ames medium) in the cell-attached mode (voltage-clamp). By convention, depolarizing responses in voltage clamp are depicted as downward deflections, and hyperpolarizing responses are upward. Thus, action potentials consist of a downward then upward deflection. Slides were perfused at 4 ml/min. Electric stimulation was used to deliver 3 ms cathodal (depolarizing) pulses to a 100 kΩ Pt-Ir stimulating electrode (Microprobes) that was centered 25 μm above the soma of targeted cells; such pulses are known to effectively initiate action potentials in a wide range of neurons. Identical anodic pulses were delivered 100 ms after the cathodal pulse to prevent charge build up on the cells or electrode; the large temporal separation between the cathodal and anodal phases allowed the response to the cathodal phase to be studied in isolation. Pulse amplitudes ranged from 0 – 20 μA; five repeats were delivered at each amplitude level. Pulse stimuli were controlled by Multi-Channel Systems STG2004 hardware and software using custom software written in LabView (National Instruments) and Matlab (Mathworks) by Maesoon Im and Daniel Freeman. Two silver chloride-coated silver wires served as the return; each was positioned ~8 mm from the targeted cell and ~6 mm from the other. Because the residual artifact(s) limited the ability to precisely determine the onset timing of the action potential, we used the peak of the depolarizing phase to compare latencies of different spikes. Threshold was determining by fitting a sigmoidal curve to the raw data points and then determining the amplitude for which there was a 50% probability of eliciting a spike. Large electrical artifacts occurred at the onset and offset of the stimulus were removed via digital filtering. Electrical stimulus artifacts arising from the cathodal pulses were removed by subtracting the inverted artifact arising from the corresponding anodic pulse. In most cases, this completely eliminated the artifact (Fig 6D). In some cases, however, there were slight temporal differences in the kinetics between the cathodal and anodal artifacts resulting in some remaining artifact (Fig 6E).

RESULTS

Increased Expression of Ephrin-A3 with Retinal Maturation

To address whether ephrin-As are negative regulators of the neurogenic potential of CE-derived cells, we examined the temporal and spatial patterns of ephrin-A3 expression in the CE and retina of the mouse eye. Quantitative analysis of western blots revealed an upregulation of ephrin-A3 beginning at postnatal day 4 (P4) in the mouse retina, reaching a peak in the adult (Fig. 1A). This temporal pattern of ephrin-A3 expression was confirmed by immunolabeling of ephrin-A3 in retinal and CE sections (Supplemental Fig. 1 & Supplemental Fig. 2), which further demonstrated that ephrin-A3 was highly expressed in the retina and CE of adult mice. The increase of ephrin-A3 expression coincides with the reduction of RSC proliferation and cessation of retinogenesis in the developing mouse retina, supporting that ephrin-A3 may send a prohibitory signal for the neurogenic program of RSCs.

Increased Proliferation of CE-derived RSCs in the Absence of Ephrin-A3

The initial step toward the regenerative response by CE-derived cells in lower vertebrates is to reenter the cell cycle. To investigate whether ephrin-A3 suppresses the potential of CE-derived cells to display stem cell properties and turn into RSCs, we first examined their ability to proliferate or reenter the cell cycle *in vivo* in the absence of ephrin-A3, using ephrin-A3 deficient mice. Following a 7-day administration of BrdU, few proliferating or BrdU+ cells were detected in either the CE or retinas of wild-type mice (Fig. 1B,C). In contrast, in adult ephrin-A3$^{-/-}$ mice, BrdU+ cells were consistently detected in both the CE (Fig. 1D) and peripheral retina (Fig. 1E). There was a greater than 20-fold increase in the number of BrdU+ cells in the CE and peripheral retinal sections (Fig. 1B) of adult ephrin-A3$^{-/-}$ mice (n=9) as compared to that of wild-type mice (n=9). Among them, approximate 95 % of BrdU+ cells were colocalized with retinal progenitor cell marker Chx10 [24] (Fig. 1F-I), suggesting their origin as proliferating RSCs. Most BrdU+ cells were non-pigmented, while a small percentage of them were seen with pigments; however, no BrdU+ cells were detected from the central retina and RPE of ephrin-A3$^{-/-}$ mice, implicating distinctive mechanisms that govern the proliferation of CE-derived cells and the remaining RPE.

To corroborate this finding, we compared the ability of CE-derived cells of wild-type and ephrin-A3$^{-/-}$ mice to form NS *in vitro* (Fig. 2A,B). Cells taken from the CE of wild-type and ephrin-A3$^{-/-}$ mice were dissociated and cultured at a single cell density for 14 days. After 7 days of incubation, we observed a significantly greater number of primary NS in cultures derived from ephrin-A3$^{-/-}$ mice than those from wild-type mice (Fig. 2). To examine secondary NS formation, primary NS were dissociated and seeded in a 24-well plate at a density of single cell colony. After 14 days of incubation, cultures of ephrin-A3$^{-/-}$ CE-derived cells displayed a 2-fold increase in number of secondary NS when compared with cultures of wild-type mice (Fig. 2F). To confirm that the increased number of NS in cultures of ephrin-A3$^{-/-}$ mice was a result of the enhanced proliferative potential of RSCs, we performed a BrdU incorporation assay (Fig. 2C, D). A 4-hour BrdU pulse stimulation yielded a significantly higher ratio of BrdU incorporation in dissociated cell cultures of NS derived from ephrin-A3$^{-/-}$ mice than those from wild-type mice (Fig. 2G), further indicating enhanced RSC proliferation in the absence of ephrin-A3. In another series of experiments, antibody-clustered ephrin-A3, which is known to activate receptor signaling [18], was added to dissociated NS cell cultures derived from wild-type mice. Administration of antibody-clustered ephrin-A3 significantly inhibited BrdU incorporation in culture as compared to untreated controls or cultures treated with control Fc (Fig. 2H). Together, these data demonstrate that ephrin-A3 negatively regulates RSC proliferation *in vivo* and *in vitro*.

Increased Neural and Photoreceptor Cell Potency in the Absence of Ephrin-A3

To further address the role of ephrin-A3 in the neurogenic potential of CE-derived RSCs, we compared the levels of expression of neural progenitor cell markers in CE-derived NS taken from wild-type and ephrin-A3$^{-/-}$ mice, using real-time RT-PCR. In the absence of ephrin-A3 signal, the expression of retinal progenitor cell marker Chx10 [23] was significantly upregulated as compared with that of wild-type mice (Fig. 3A). There was also an overall increase in the expression of neural progenitor cell markers Ngn2, Sox2, Math5 and Math1, and photoreceptor precursor cell markers Crx, Nrl and Nr2e3 [24], in CE-derived NS cells of ephrin-A3$^{-/-}$ mice than in wild-type mice (Fig. 3B-D). These data were supported by the drastic upregulation of neurogenic signals, such as the Wnt family members (e.g. Wnt1, Wnt3a and Wnt7a), in NS cells derived from ephrin-A3$^{-/-}$ mice as compared to those from wild-type mice (Fig. 3C,D). In contrast, expression of the pigment epithelial progenitor cell marker Mift [25] was significantly downregulated in NS taken from ephrin-A3$^{-/-}$ mice, implicating a decreased pigment epithelial cell potency when the cells exhibited enhanced

retinal progenitor cell fate. The data suggest that expression of ephrin-A3 in CE-derived cells inversely correlates with their neural progenitor cell potency.

To investigate if CE-derived RSCs of ephrin-A3$^{-/-}$ mice display increased potency to generate retinal neurons and photoreceptors, NS cells of wild-type and ephrin-A3$^{-/-}$ mice were induced to differentiate in culture. Following 7 days of incubation, CE-derived NS cells gradually lost pigmentation and exhibited a morphology that differs from the CE (Fig. 4A, B). By 21 days, CE-derived NS cells taken from ephrin-A3$^{-/-}$ mice differentiated into various types of retinal cells. These cells expressed retina-specific cell markers, such as GFAP (glial cell marker – 73.21 ± 10.22%), recoverin (rod photoreceptor cell marker – 24.66 ± 4.32%), β-III-tublin (Tuj; neuronal marker – 1.51 ± 0.28%), and MAP2 (mature neuron marker – 1.01 ± 0.21%), and exhibited corresponding neuronal and glial cell morphologies (Fig. 4C-I). In contrast, very few NS cells of wild-type mice were found to express the retinal neuron markers mentioned above after 21 days of incubation, suggesting their limited ability to differentiate into retina-specific cells. Quantitative analysis with real-time RT-PCR confirmed that following incubation RSCs of both wild-type and ephrin-A3$^{-/-}$ mice downregulated retinal progenitor cell markers Pax6 and Chx10 (Fig. 5A). However, after 10 days of incubation, cultures derived from ephrin-A3$^{-/-}$ mice exhibited significantly higher levels of expression of retinal neuron and glial markers, such as rhodopsin, recoverin, PKCα and GFAP, indicating increased photoreceptor and retinal cell potency than in cultures from wild-type mice (Fig. 5B).

To determine if ephrin-A3 promotes an RPE cell fate while suppressing the neuronal fate, NS cells of wild-type mice were cultured in the presence of control Fc or antibody clustered form of ephrin-A3. Following 7 day induction of differentiation, CE-derived NS cells treated with antibody clustered form of ephrin-A3 exhibited significantly higher number of pigmented cells as compared to control Fc treated cultures. The percentage of pigmented cells doubled in ephrin-A3 treated group as compared to the control group (Fig. 5C), suggesting that ephrin-A3 promotes the RPE progeny of CE-derived RSCs while suppresses RSC proliferation.

To verify the functional capacity of neurons differentiated from CE-derived RSCs of ephrin-A3$^{-/-}$ mice, next we measured the response of post differentiated neurons to extracellular electric stimulation, which method effectively elicits action potentials in a wide range of neurons [25, 26]. At 1, 3 and 5 weeks post differentiation, RSCs with round cell bodies and axon-like neurites were recorded, and a patch-clamp electrode in cell-attached mode was established on the soma in order to record the cell's spiking response to stimulation. A small stimulating electrode was positioned ~25 μm above the soma of the targeted cells. Cathodal pulses, with duration of 3 ms and amplitudes ranging from 0-20 μA were delivered at a rate of 1 Hz. Responses recorded from a typical cell at 3 week posted differentiation are shown in Figure 5D: the positive responses consisted of biphasic waveforms that are characteristics of action potential propagation; they exhibited an excitatory (downward) current with ~0.5 ms duration followed immediately by an inhibitory (upward) current that persisted for ~1 ms. Similar responses were found in 13/13 cells recorded, suggesting their maturation into functional neurons. As expected, the likelihood of eliciting a spike increased with the amplitude of stimulation (Fig. 5E,F). Response threshold (defined as the amplitude for which 50% of pulses elicited action potentials), was measured in 11 cells (2/13 cells displayed only a single amplitude). Among these 11 cells, we noted 2 types of cell populations: Type A with a mean value of 2.99 μA (n= 5/11) and Type B with a mean value of 9.07 μA (n=6/11; P=0.00597). Both types of responses had been detected in mature retinal neurons, and the lower thresholds in type A neurons suggest a higher concentration of sodium channels. Consistent with previous studies of spiking neurons [25, 26], the latency of spike onset decreased with increasing stimulus amplitude (Fig. 5E, G), further supporting

the voltage-dependent ion channel activities in these neurons. Like early differentiated neurons, all of the 13 RSCs examined at 3 weeks post differentiation also exhibited rhythmic spontaneous discharges (Fig. 5D, bottom row) at an average frequency of ~0.3 Hz, with inward currents that were smaller and slightly shorter in duration than the depolarizing phase of action potentials. Spontaneous currents disappeared in RSCs that were differentiated for 5 weeks (n=5), similar to that is seen in mature retinal neurons. Whereas, spontaneous inward currents could be detected in all RSCs at 1 week post differentiation, when no action potentials could be elicited from these younger cells (n=16). Thus, neuron-like cells differentiated from CE-derived RSCs of ephrin-A3$^{-/-}$ mice showed major electrophysiological characteristics of typical retinal neurons in terms of spontaneous spiking activity [27, 28], temporal parameters of mature action potentials and voltage-dependent currents, which gradually developed in a time-dependent manner. In contrast, no action potential-related transient current were ever detected from astroglia-like cells, which exhibited large flat somas with no visible elongated processes (not shown). Together, these data indicate that ephrin-A3 is a negative regulator of the neurogenic potential for CE-derived RSCs which shift the cells toward a pigment epithelial cell fate.

Ephrin-A3 Functioning through EphA4 and the Suppression of Wnt Signaling to Regulate the Neurogenic Potential of CE-derived RSCs

Our previous research showed that ephrin-A3 acts, at least in part, through forward signaling to cause neural stem cell growth inhibition [18]. EphA4 and EphA7 were reported to be the primary receptors of ephrin-A3; therefore, in this study we examined the expression of EphA4 and EphA7 in CE-derived NS cells, using immunohistochemistry and RT-PCR. Immunodetection revealed EphA4 (Fig. 6A, B), but not EphA7 (data not shown), in the CE. Results of RT-PCR further confirmed that EphA4 is prominently expressed by CE-derived RSCs (Fig. 6C). Immunoprecipitation of cell lysates taken from the CE with the ephrin-A3 antibody also pulled down EphA4, instead of EphA7, supporting the notion that EphA4 is the predominant ephrin-A3 receptor in CE-derived cells (Fig. 6B). In agreement with those findings, Western blot analysis detected EphA4 activation and phosphorylation in cell lysates taken from the ciliary bodies of wild-type, but not ephrin-A3$^{-/-}$ mice (Fig. 6E). To further demonstrate that ephrin-A3 functions through the EphA4 receptor, we performed a BrdU incorporation assay using CE-derived NS cell cultures (Fig. 6F). Following a 4-hour BrdU pulse stimulation, 36% of NS cells derived from the CE of wild-type mice became BrdU+. Addition of soluble EphA4 protein, which competes and inhibits the activity of intrinsic EphA4 receptors, but not its control Fc, significantly increased BrdU-incorporation into NS cells in culture, supporting a role for EphA4 as the functional receptor of ephrin-A3 to mediate CE-derived NS cell proliferation (Fig. 6F).

Several lines of evidence suggest that Wnt3a/β-catenin signaling plays pivotal roles in the neurogenic potential of neural stem cells [30-32]. The fact that CE-derived RSCs of ephrin-A3$^{-/-}$ mice had increased levels of Wnts (Fig. 3D) prompted us to ask whether the Wnt pathway is critically involved as a downstream target of ephrin-A3 to mediate the proliferative potential of RSCs. To test this, we examined expression of the canonical downstream pathway of Wnt3a signaling, β-catenin. We noted an average 4-fold increase in β-catenin level in primary CE-derived NS cells of ephrin-A3$^{-/-}$ mice as compared to that of wild-type mice (Fig. 7A, B), strongly suggesting increased activation of the canonical Wnt pathway. In the BrdU incorporation assay, addition of Wnt3a into the culture resulted in greater than 2-fold increase in BrdU incorporation into CE-derived NS cells of wild-type mice as compared to the untreated control group (Fig. 7C-E). Together, the results suggest that ephrin-A3 functions through EphA4 to present a negative niche for the proliferation and neurogenic potential of CE-derived RSCs by suppressing Wnt/β-catenin signaling.

DISCUSSION

This study identifies ephrin-A3 as a key inhibitor of retinal stem cell potency and neuronal fate of CE-derived RSCs in the adult mouse. Absence of ephrin-A3 enhances the proliferation of CE-derived RSCs *in vivo*. However, the number of BrdU+ cells migrating into the retina of ephrin-A3$^{-/-}$ mice remained low, and even fewer was found to differentiate and express a retinal neuron marker (e.g. rhodopsin or β-III-tubulin), suggesting an extremely low neurogenic potential in these mice *in vivo*. In part, this may be caused by the presence of other negative niche signals, such as ephrin-A2 [18], in the microenvironments of the adult CE and retina. In the future, it would be interesting to determine if absence of both ephrin-A2 and -A3 further enhances the neurogenic potential of CE-derived RSCs *in vivo*.

CE-derived cells are of neuroepithelial origin and thought to possess both epithelial and neural progenitor cell properties. It has been previously reported that these cells express neuronal progenitor markers Chx10 and nestin and are intrinsically capable of generating retina-specific neurons *ex vivo*. However, it was recently reported that CE-derived cells exhibit primarily pigmented epithelial cell properties, with little neurogenic potential [10] and limited ability to differentiate into photoreceptors [11]. On the basis of our data, we propose a working model for how the neurogenic potential of CE-derived RSCs is regulated. We suggest that CE-derived cells maintain a balance between epithelial and neurogenic potential in the adult. This balance is controlled by 2 intrinsically linked but opposing signaling events—the inhibitory and stimulatory neurogenic signals the cell receives. Ephrin-A3/EphA4 pathways comprise the inhibitory signals that suppress retinal progenitor maintenance, while the Wnt pathways promote the proliferation and neuronal fate of CE-derived cells. Interactions between ephrin and Wnt pathways can also be found in several other progenitor/stem cell systems; these include small intestine stem cells [33-35] and the developing xenopus optic tectum [36]. The list of negative and positive regulators is likely to grow as the mechanisms underlying the actions and interactions of these pathways are unveiled. Cross talk between these pathways imposes both positive and negative feedback regulation, enabling better response to environmental cues and providing a level of plasticity in regulation in the adult mouse.

While the CE is composed of 2 layers of cuboidal cells—pigmented and nonpigmented cells, ephrin-A3 and EphA4 were detected in almost all cells of both layers. It has been shown that both ephrins and Eph family receptor tyrosine kinases are expressed by neural progenitors [18, 20, 37]. While ephrins can mediate a bidirectional signaling [38], our experiments using soluble EphA4 protein, which competes and inhibits the activity of intrinsic EphA4 receptors, strongly suggest that ephrin-A3 evokes an EphA4 forward signal to suppress the proliferation of CE-derived RSCs. We propose that the niche cells in the CE constantly interact with RSCs *in vivo* by making direct contact to inhibit their neurogenic potential.

Ephrin family proteins act in combination with an Eph receptor are pivotal regulators of CNS development, including axon guidance, neural migration and patterning, synapse formation, and vascular morphogenesis [39, 40]. Recent studies also point to a role for ephrin families functioning as inhibitors of neurogenesis in the subgranular zone and other brain areas of adult mice [18]. Results in the present study support the premise that ephrin-As are also involved in the regulation of the neurogenic potential of RSCs. Expression of ephrin-A3 increases as the retina matures, along with the cessation of RSC proliferation and retinogenesis [3]. In adult retina and CE, expression of ephrin-A3 is high, and its absence results in increased proliferation of RSCs in the CE and peripheral retina—a margin reminiscent of the ciliary marginal zone of fish and amphibians [3, 41-43]. These data

suggest that ephrin-A3 is a component of an inhibitory niche for adult RSCs in mice. In agreement with previous reports [2], we found that CE-derived RSCs of ephrin-A3$^{-/-}$ mice are initially pigmented, but then undergo a course of depigmentation. Moreover, expression of pigmented epithelial progenitor marker Mitf was downregulated before RSCs transformed into retinal neural progenitors in culture. These progenitor cells subsequently downregulated RSC markers Chx10 and Pax6 during differentiation. Also consistent with previous reports [2, 9-11], we show that the potential of CE-derived cells of wild-type mice to differentiate into photoreceptors or other retina-specific cells is negligible. However, RSCs derived from ephrin-A3$^{-/-}$ mice consistently exhibited drastic upregulation of the expression of photoreceptor progenitor cell markers Crx, Nr2e3 and Nrl, as compared to that of wild-type mice, and enhanced potency to differentiate into retinal neurons and photoreceptor cells. These data suggest that adult CE-derived cells possess the machinery or properties of retinal progenitor cells; however, their neuro- and retinogenic potential is negatively regulated by ephrin-A3 signaling under normal adult conditions. Thus, manipulating the ephrin-A3 signaling pathway may present a viable approach to redirecting CE-derived cells toward a retinal progenitor cell fate.

The present work also contributes to resolving an issue regarding the function of and signaling events associated with ephrin-A3 in adult stem cell regulation. While EphA7 and EphA4 are reported to serve as the receptors of ephrin-A3 [18, 19, 21, 44, 45], our data suggest that ephrin-A3 primarily binds EphA4 in the CE, to suppress the activity and expression of Wnt3a/β-catenin pathways and, in turn, mediate the neurogenic potential of adult RSCs. At this point, we cannot rule out the possibility that ephrin-A3 and EphA4 also act bidirectionally to regulate the behavior of adult RSCs. Interconnection between the ephrin and Wnt pathways has been previously reported, where ephrin-B1 was shown to inhibit the Wnt3a/β-catenin pathway through binding to EphB receptors [35]. Here we report that ephrin-A3 activates EphA4 to suppress Wnt3a/β-catenin signaling, and that addition of Wnt3a alone is sufficient to promote cell proliferation. RSCs derived from ephrin-A3$^{-/-}$ mice showed significantly increased levels of expression of Wnt family members, including Wnt1, Wnt3a and Wnt7 (Fig. 4D), and their downstream signal β-catenin. While ideally, activation of Wnt/β-catenin signal should be examined by comparing the free β-catenin levels in relation to total β-catenin levels in the cells, this experiment is technically difficult as each mouse contains only limited number of CE-derived RSCs. Alternatively, we were able to show that the total β-catenin levels in RSCs of ephrin-A3$^{-/-}$ mice were drastically upregulated as compared to wild-type mice, suggesting increased β-catenin stability and activation of Wnt signaling. These observations are in agreement with a previous report demonstrating increased number and size of primary and secondary NS in CE-derived cell cultures stimulated by Wnt3a [15]. Together our data support a negative role for ephrin-A3 in the Wnt pathways. Among the neurogenic signals examined, we also noted drastic upregulation of Ngn1, Sox2, Math1 and Math5 in CE-derived RSCs of ephrin-A3$^{-/-}$ mice as compared to wild-type mice, suggesting involvement and complex interactions among multiple signaling pathways. While further experiments are needed to unravel the molecular details of these interactions, together, our results suggest that the interactions and balance between ephrin-A3 and Wnt/β-catenin pathways mediates retinal progenitor cell potency in adult CE.

Conclusion

Our study demonstrates ephrin-A3 as a key component of the adult retinal stem cell niche, which acts through EphA4 to suppress Wnt signaling and inhibit the neurogenic potential of CE-derived RSCs. Deletion of ephrin-A3 increases the proliferation and expression of neural retinal progenitor cell genes, as well as photoreceptor potency for CE-derived RSCs while presence of ephrin-A3 suppresses the neurogenic potential and shift CE-derived cells

toward a pigment epithelial cell fate. Despite the fact that the CE is easily obtained in humans by a minimally invasive procedure, to date, the clinical promise of CE-derived RSCs serving as an endogenous source of retinal neural progenitors for the treatment of photoreceptor damage or degenerative disorders is yet to be realized. However, this potential avenue for treatment can only be fully explored with a comprehensive understanding of the mechanisms and molecular signals that control the cellular properties and differentiation of CE-derived cells.

Supplementary Material

Refer to Web version on PubMed Central for supplementary material.

Acknowledgments

The project was supported by grants from NIH/NEI (R01EY017641), NIDA (R21DA024803), Department of Veterans Affairs (1I01RX000110), Department of Defense (W81XWH-09-2-0091) to D. F. C., Lion's Foundation Grant to K-S C., the National Basic Research Program of China (No. 2007CB512204) to X. S. and National Natural Science Foundation (NSFC81100667) to Y. F.

REFERENCES

1. Lamba DA, Karl MO, Reh TA. Strategies for retinal repair: cell replacement and regeneration. Prog Brain Res. 2009; 175:23–31. [PubMed: 19660646]
2. Tropepe V, Coles BL, Chiasson BJ, et al. Retinal stem cells in the adult mammalian eye. Science. 2000; 287:2032–2036. [PubMed: 10720333]
3. Kubota R, Hokoc JN, Moshiri A, et al. A comparative study of neurogenesis in the retinal ciliary marginal zone of homeothermic vertebrates. Brain Res Dev Brain Res. 2002; 134:31–41.
4. Araki M. Regeneration of the amphibian retina: role of tissue interaction and related signaling molecules on RPE transdifferentiation. Dev Growth Differ. 2007; 49:109–120. [PubMed: 17335432]
5. Reh TA, Nagy T, Gretton H. Retinal pigmented epithelial cells induced to transdifferentiate to neurons by laminin. Nature. 1987; 330:68–71. [PubMed: 3499570]
6. MacNeil A, Pearson RA, MacLaren RE, et al. Comparative analysis of progenitor cells isolated from the iris, pars plana, and ciliary body of the adult porcine eye. Stem Cells. 2007; 25:2430–2438. [PubMed: 17600111]
7. Coles BL, Angenieux B, Inoue T, et al. Facile isolation and the characterization of human retinal stem cells. Proc Natl Acad Sci U S A. 2004; 101:15772–15777. [PubMed: 15505221]
8. Xu H, Sta Iglesia DD, Kielczewski JL, et al. Characteristics of progenitor cells derived from adult ciliary body in mouse, rat, and human eyes. Invest Ophthalmol Vis Sci. 2007; 48:1674–1682. [PubMed: 17389499]
9. Nishiguchi KM, Kaneko H, Nakamura M, et al. Identification of photoreceptor precursors in the pars plana during ocular development and after retinal injury. Invest Ophthalmol Vis Sci. 2008; 49:422–428. [PubMed: 18172121]
10. Cicero SA, Johnson D, Reyntjens S, et al. Cells previously identified as retinal stem cells are pigmented ciliary epithelial cells. Proc Natl Acad Sci U S A. 2009; 106:6685–6690. [PubMed: 19346468]
11. Gualdoni S, Baron M, Lakowski J, et al. Adult ciliary epithelial cells, previously identified as retinal stem cells with potential for retinal repair, fail to differentiate into new rod photoreceptors. Stem Cells. 2010; 28:1048–1059. [PubMed: 20506130]
12. Zhao X, Das AV, Soto-Leon F, et al. Growth factor-responsive progenitors in the postnatal mammalian retina. Dev Dyn. 2005; 232:349–358. [PubMed: 15637695]
13. Abdouh M, Bernier G. In vivo reactivation of a quiescent cell population located in the ocular ciliary body of adult mammals. Exp Eye Res. 2006; 83:153–164. [PubMed: 16563378]

14. Kubo F, Nakagawa S. Hairy1 acts as a node downstream of Wnt signaling to maintain retinal stem cell-like progenitor cells in the chick ciliary marginal zone. Development. 2009; 136:1823–1833. [PubMed: 19386663]
15. Inoue T, Kagawa T, Fukushima M, et al. Activation of canonical Wnt pathway promotes proliferation of retinal stem cells derived from adult mouse ciliary margin. Stem Cells. 2006; 24:95–104. [PubMed: 16223856]
16. De Marzo A, Aruta C, Marigo V. PEDF promotes retinal neurosphere formation and expansion in vitro. Adv Exp Med Biol. 2010; 664:621–630. [PubMed: 20238066]
17. Inoue T, Coles BL, Dorval K, et al. Maximizing functional photoreceptor differentiation from adult human retinal stem cells. Stem Cells. 2010; 28:489–500. [PubMed: 20014120]
18. Jiao JW, Feldheim DA, Chen DF. Ephrins as negative regulators of adult neurogenesis in diverse regions of the central nervous system. Proc Natl Acad Sci U S A. 2008; 105:8778–8783. [PubMed: 18562299]
19. Martinez A, Soriano E. Functions of ephrin/Eph interactions in the development of the nervous system: emphasis on the hippocampal system. Brain Res Brain Res Rev. 2005; 49:211–226. [PubMed: 16111551]
20. Depaepe V, Suarez-Gonzalez N, Dufour A, et al. Ephrin signalling controls brain size by regulating apoptosis of neural progenitors. Nature. 2005; 435:1244–1250. [PubMed: 15902206]
21. Holmberg J, Armulik A, Senti KA, et al. Ephrin-A2 reverse signaling negatively regulates neural progenitor proliferation and neurogenesis. Genes Dev. 2005; 19:462–471. [PubMed: 15713841]
22. Jiao J, Chen DF. Induction of neurogenesis in nonconventional neurogenic regions of the adult central nervous system by niche astrocyte-produced signals. Stem Cells. 2008; 26:1221–1230. [PubMed: 18323412]
23. Moe MC, Kolberg RS, Sandberg C, et al. A comparison of epithelial and neural properties in progenitor cells derived from the adult human ciliary body and brain. Exp Eye Res. 2009; 88:30–38. [PubMed: 18955049]
24. Oh EC, Khan N, Novelli E, et al. Transformation of cone precursors to functional rod photoreceptors by bZIP transcription factor NRL. Proc Natl Acad Sci U S A. 2007; 104:1679–1684. [PubMed: 17242361]
25. Fried SI, Lasker AC, Desai NJ, et al. Axonal sodium-channel bands shape the response to electric stimulation in retinal ganglion cells. J Neurophysiol. 2009; 101:1972–1987. [PubMed: 19193771]
26. Tehovnik EJ, Tolias AS, Sultan F, et al. Direct and indirect activation of cortical neurons by electrical microstimulation. J Neurophysiol. 2006; 96:512–521. [PubMed: 16835359]
27. Soto F, Ma X, Cecil JL, et al. Spontaneous activity promotes synapse formation in a cell-type-dependent manner in the developing retina. J Neurosci. 2012; 32:5426–5439. [PubMed: 22514306]
28. Blankenship AG, Feller MB. Mechanisms underlying spontaneous patterned activity in developing neural circuits. Nat Rev Neurosci. 2010; 11:18–29. [PubMed: 19953103]
29. Osakada F, Ikeda H, Sasai Y, et al. Stepwise differentiation of pluripotent stem cells into retinal cells. Nat Protoc. 2009; 4:811–824. [PubMed: 19444239]
30. Lie DC, Colamarino SA, Song HJ, et al. Wnt signalling regulates adult hippocampal neurogenesis. Nature. 2005; 437:1370–1375. [PubMed: 16251967]
31. Kunke D, Bryja V, Mygland L, et al. Inhibition of canonical Wnt signaling promotes gliogenesis in P0-NSCs. Biochem Biophys Res Commun. 2009; 386:628–633. [PubMed: 19545542]
32. Wexler EM, Paucer A, Kornblum HI, et al. Endogenous Wnt signaling maintains neural progenitor cell potency. Stem Cells. 2009; 27:1130–1141. [PubMed: 19418460]
33. Clarke AR. Wnt signalling in the mouse intestine. Oncogene. 2006; 25:7512–7521. [PubMed: 17143295]
34. Wei S, Xu G, Bridges LC, et al. ADAM13 induces cranial neural crest by cleaving class B Ephrins and regulating Wnt signaling. Dev Cell. 2010; 19:345–352. [PubMed: 20708595]
35. Batlle E, Henderson JT, Beghtel H, et al. Beta-catenin and TCF mediate cell positioning in the intestinal epithelium by controlling the expression of EphB/ephrinB. Cell. 2002; 111:251–263. [PubMed: 12408869]

36. Lim BK, Cho SJ, Sumbre G, et al. Region-specific contribution of ephrin-B and Wnt signaling to receptive field plasticity in developing optic tectum. Neuron. 2010; 65:899–911. [PubMed: 20346764]
37. Greferath U, Canty AJ, Messenger J, et al. Developmental expression of EphA4-tyrosine kinase receptor in the mouse brain and spinal cord. Mech Dev. 2002; 119(Suppl 1):S231–238. [PubMed: 14516691]
38. Cowan CA, Henkemeyer M. Ephrins in reverse, park and drive. Trends Cell Biol. 2002; 12:339–346. [PubMed: 12185851]
39. Egea J, Klein R. Bidirectional Eph-ephrin signaling during axon guidance. Trends Cell Biol. 2007; 17:230–238. [PubMed: 17420126]
40. Klein R. Bidirectional modulation of synaptic functions by Eph/ephrin signaling. Nat Neurosci. 2009; 12:15–20. [PubMed: 19029886]
41. Moshiri A, Reh TA. Persistent progenitors at the retinal margin of ptc+/- mice. J Neurosci. 2004; 24:229–237. [PubMed: 14715955]
42. Marquardt T, Ashery-Padan R, Andrejewski N, et al. Pax6 is required for the multipotent state of retinal progenitor cells. Cell. 2001; 105:43–55. [PubMed: 11301001]
43. Lamba D, Karl M, Reh T. Neural regeneration and cell replacement: a view from the eye. Cell Stem Cell. 2008; 2:538–549. [PubMed: 18522847]
44. Carmona MA, Murai KK, Wang L, et al. Glial ephrin-A3 regulates hippocampal dendritic spine morphology and glutamate transport. Proc Natl Acad Sci U S A. 2009; 106:12524–12529. [PubMed: 19592509]
45. Filosa A, Paixao S, Honsek SD, et al. Neuron-glia communication via EphA4/ephrin-A3 modulates LTP through glial glutamate transport. Nat Neurosci. 2009; 12:1285–1292. [PubMed: 19734893]

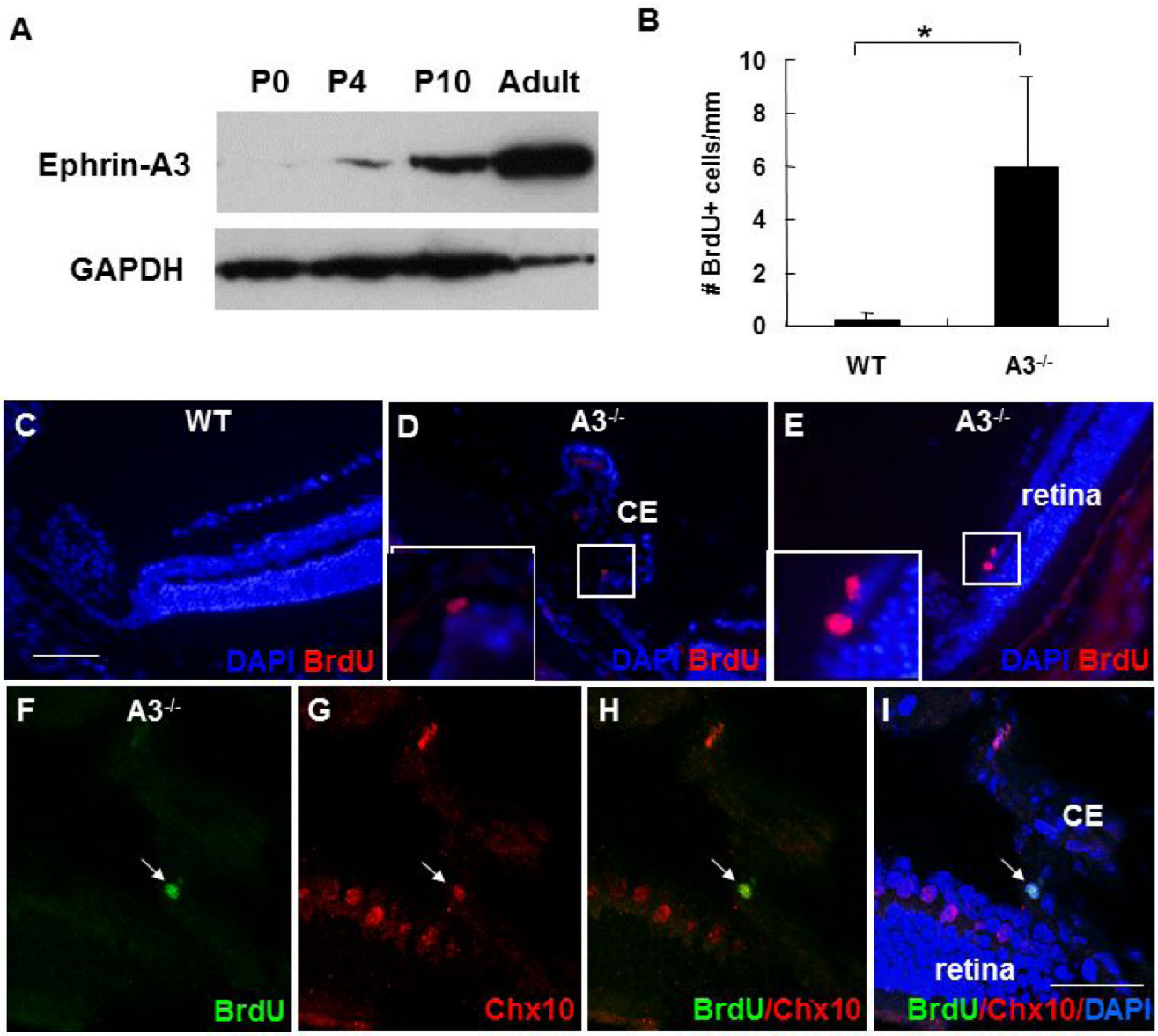

Figure 1.

Increased proliferation of RSCs in adult ephrin-A3$^{-/-}$ mice. **(A)** Representative western blots of triplicate experiments show ephrin-A3 expression in retinal tissues (including the CE) collected from mice of differing ages. Note that the expression of ephrin-A3 has begun to be detectable on postnatal day 4 (P4) and reaches its peak in the adult. **(B)** Counts of BrdU+ cells in the CE and peripheral retinas of adult wild-type (WT) and ephrin-A3$^{-/-}$ (A3$^{-/-}$) mice (* P<0.05 by Mann-Whitney Rank Sum Test; n=6/group). **(C-I)** Epifluorescence photomicrographs of retinal and CE sections of wild-type **(C)** and ephrin-A3$^{-/-}$ **(D-I)** mice were taken after a 7-day administration of BrdU. The sections were double-immunolabeled with primary antibodies against BrdU and Chx10, and were counterstained with DAPI (blue). Note the increased detection of BrdU+ cells in the peripheral retina and CE in adult ephrin-A3$^{-/-}$ mice **(E-I)** as compared to that in wild-type mice **(C)**. Note also the colocalization of BrdU+ cells with retinal progenitor cell marker Chx10 **(F-I)**, suggesting that they are retinal progenitors. Scale bar: 100 μm.

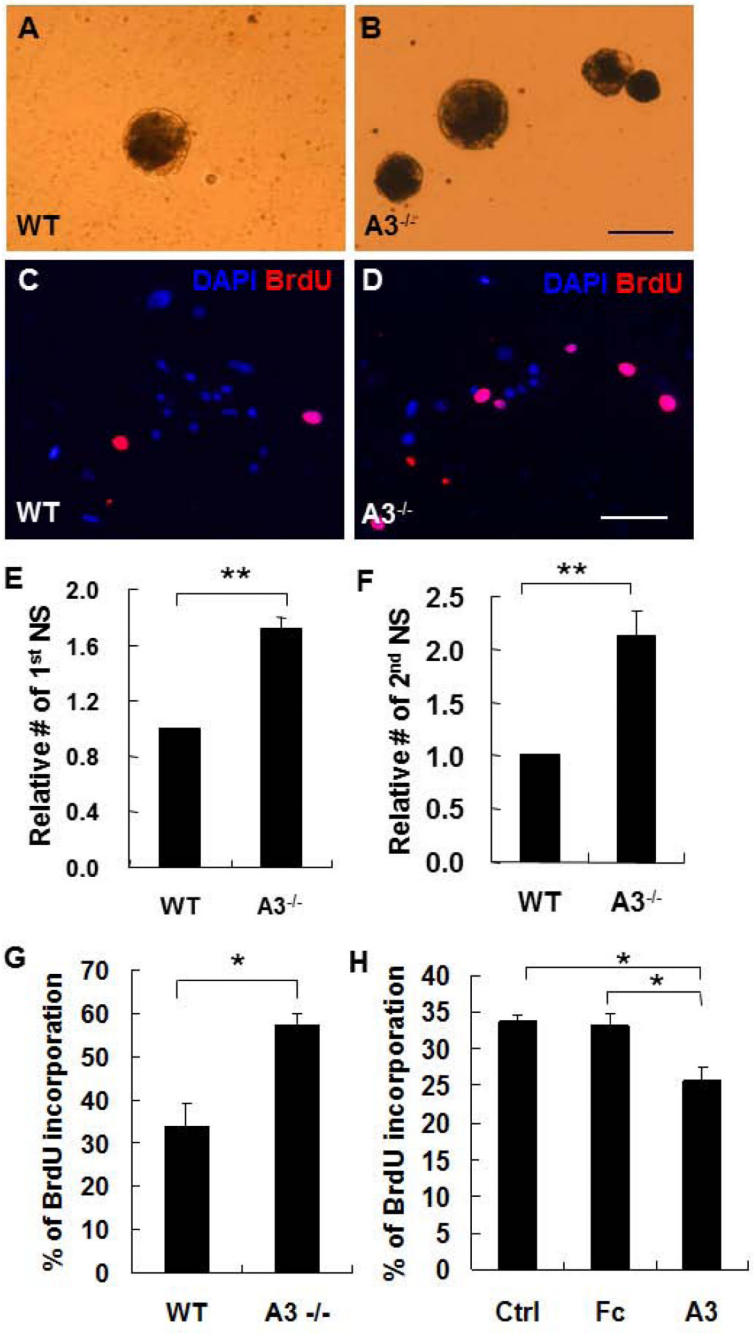

Figure 2.

Increased proliferation and NS formation in CE-derived cell cultures prepared from adult ephrin-A3$^{-/-}$ mice than that from wild-type mice. **(A,B)** Phase images show primary neurospheres (NSs) formed in CE-derived cell cultures prepared from adult wild-type **(A: WT)** and ephrin-A3$^{-/-}$ **(B:** A3$^{-/-}$**)** mice. Scale bar: 100 μm. **(C,D)** Epifluorescence images taken of NS-derived cells that were dissociated and cultured in the presence of BrdU for 24 hours before they were double-labeled by anti-BrdU (red) and DAPI (blue). Scale bar: 50 μm. **(E-H)** Quantification was performed of primary **(E)** and secondary NSs **(F)**, and percentage of BrdU incorporation **(G)** in NS-derived cell cultures prepared from wild-type

and ephrin-A3$^{-/-}$ mice, or in CE-derived cultures of wild-type mice that were either untreated (Ctrl) or treated with control Fc (Fc) or clustered ephrin-A3 (A3) **(H)**. More primary NSs developed in cultures from ephrin-A3$^{-/-}$ mice than from wild-type mice (*P<0.05; **P< 0.01; by two tailed student's t test; n=3/group).

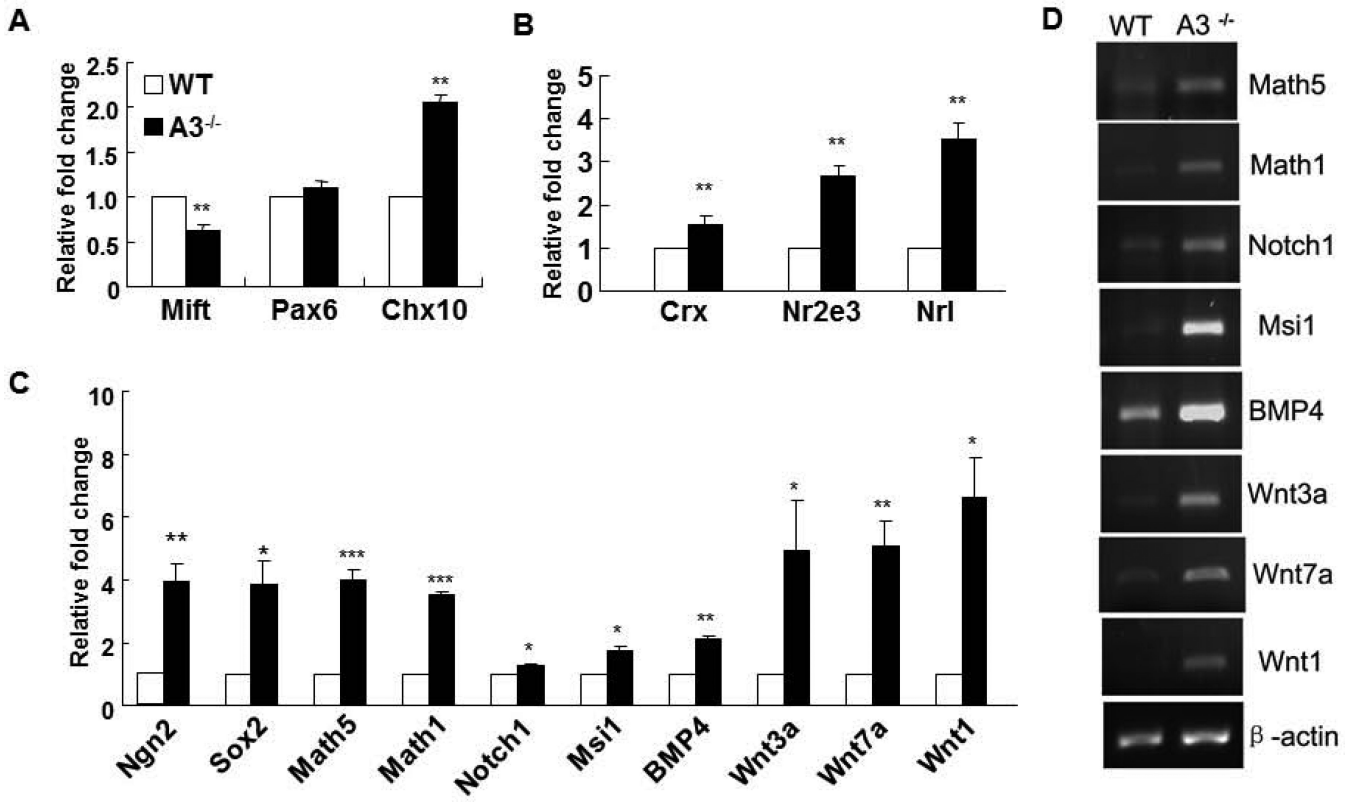

Figure 3.

RSCs of ephrin-A3$^{-/-}$ mice expressing higher levels of retinal neural progenitor cell markers. **(A-C)** Comparisons were made of expression of pigment epithelial cell marker Mift, and retinal and photoreceptor progenitor cell markers in CE-derived NS cells of wild-type and ephrin-A3$^{-/-}$ mice, using a real-time RT-PCR. (*P<0.05, **P<0.01, ***P<0.001 by two tailed student's t test or Mann-Whitney Rank Sum Test.) **(D)** Representative semi-quantitative RT-PCR of CE-derived NS cells of wild-type and ephrin-A3$^{-/-}$ mice reveals results similar to those by the real-time RT-PCR.

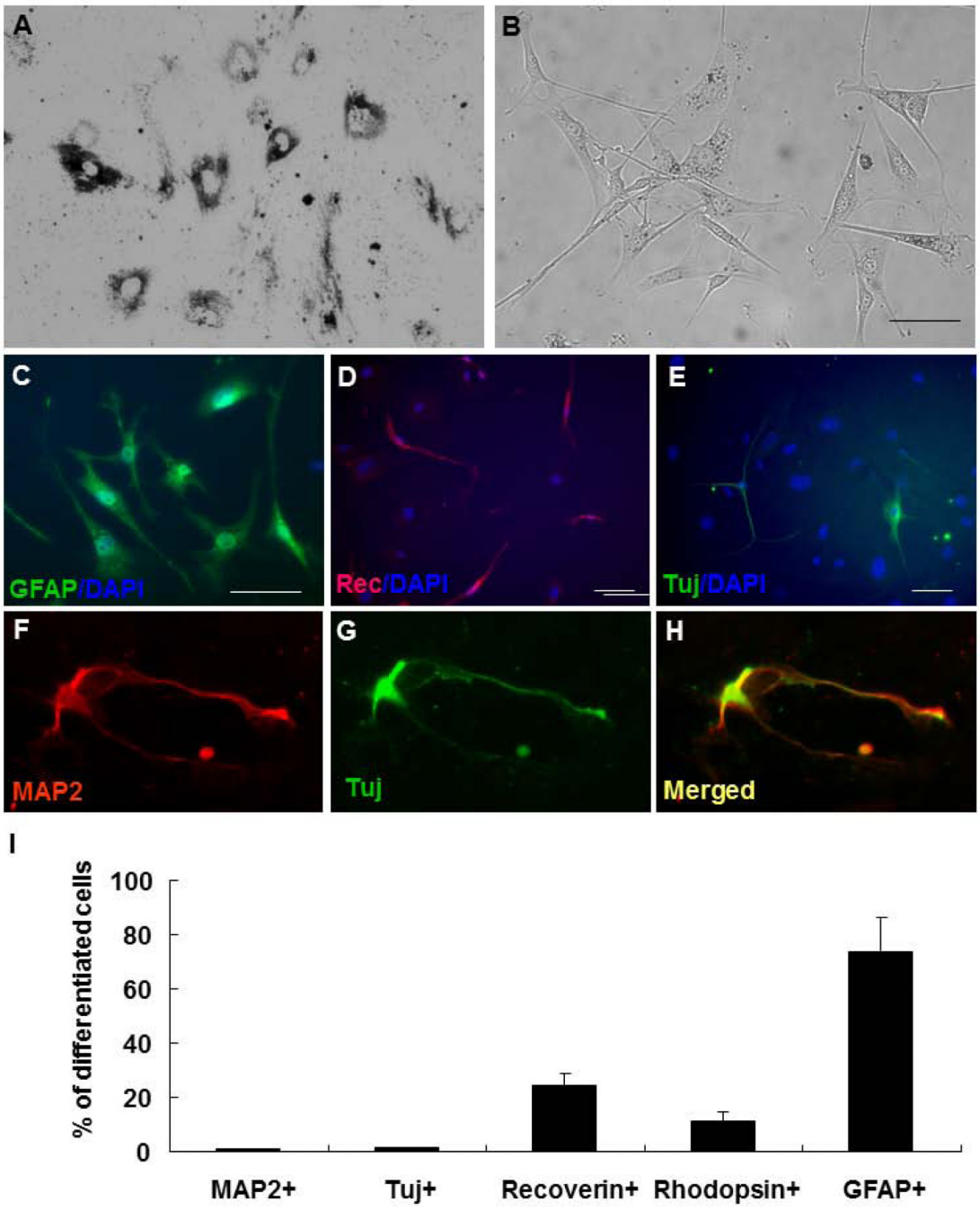

Figure 4.

Neural and glial differentiation by CE-derived RSCs of adult ephrin-A3$^{-/-}$ mice. **(A,B)** Phase images were of CE-derived NS cells taken from adult ephrin-A3$^{-/-}$ mice before **(A)** and after **(B)** they lost pigmentation and exhibited a morphology that differs from that of CE cells. **(C-E)** Epifluorescence photomicrographs represent CE-derived NS cells that were induced to differentiate for 21 days and double-labeled with DAPI and a primary antibody against a glial cell marker GFAP **(C)**, rod photoreceptor cell marker recoverin **(**Rec; **D)**, or a neuronal marker β-III-tubulin **(**Tuj; **E**). (**F-H)**, Epifluorescence images were taken of a Tuj1+ (green) neuron differentiated from CE-derived NS cells of ephrin-A3$^{-/-}$ mice show that co-expresses

the mature neuronal marker, MAP2 (red). Dissociated CE-derived NS cells from adult ephrin-A3$^{-/-}$ mice were cultured for 21 days to allow differentiation and then triple-labeled with DAPI and primary antibodies against MAP2 (red) and β-III-tubulin (Tuj; green) and then merged **(H)** Scale bar: 20 μm. **(I,)** Percentage of CE-derived RSCs expressing neural and glial cell markers following differentiation in culture.

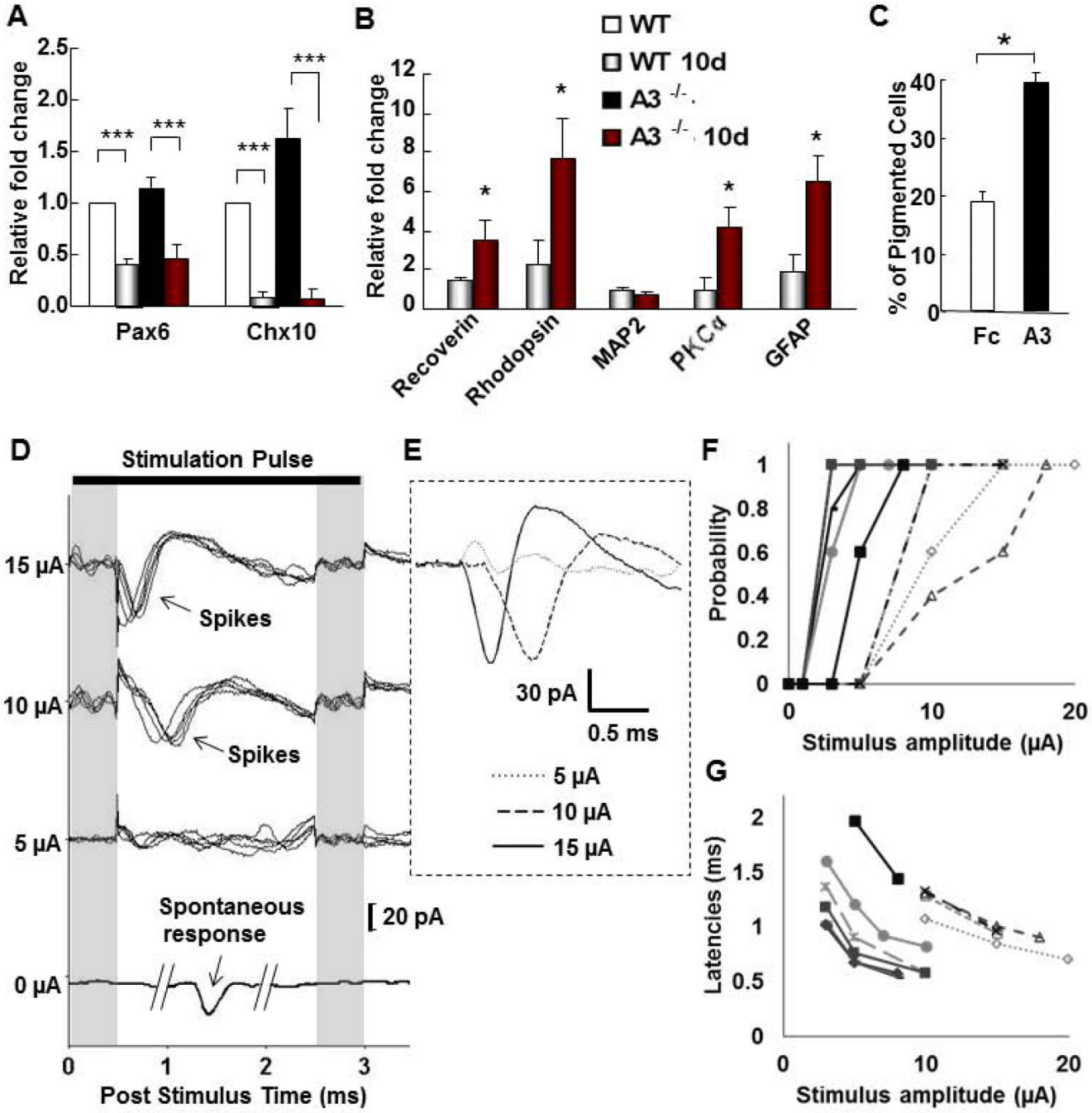

Figure 5.

Characterization of neuronal and RPE progeny of CE-derived RSCs from ephrin-A3$^{-/-}$ mice. **(A,B)** Quantitative analyses were made of mRNA expression of retinal progenitors Pax6 and Chx10, and neuronal markers in CE-derived NS cell cultures prepared from adult wild-type (WT) and ephrin-A3$^{-/-}$ (A3$^{-/-}$) mice. Real-time RT-PCR was performed in NS cells before and after induction of differentiation for 10 days (10 d), and mRNA expression levels were normalized to wild-type NS cultures before the induction of differentiation. Note the drastic reduction of expression of retinal progenitor cell markers Pax6 and Chx10 following differentiation in NS cell cultures derived from both wild-type and ephrin-A3$^{-/-}$ mice **(A)**.

Ephrin-A3 deficiency results in a significant increase in expression of retinal neuron and glial markers following differentiation **(B)**, indicating their increased retinal progenitor cell potency. **(C)** Percentage of pigmented cells in CE-derived RSC cultures that were treated with control Fc (Fc) or clustered ephrin-A3 (A3), indicating increased pigmented cell progeny induced by ephrin-A3. (*P<0.05, **P<0.01, ***P<0.001, by two tailed student's t test or Mann-Whitney Rank Sum Test; n=3/group). **(D)** Responses of post differentiatiated neurons to cathodal pulses at 3 amplitude levels. Each waveform is the isolated response (artifact subtracted) to a single pulse, and 5 repeats for each stimulus level are overlaid. Waveform at bottom is a typical spontaneously recorded inward current. Vertical shaded regions correspond to locations where the electrical artifact was digitally subtracted. **(E)** Overlay of the average responses (in D) at 3 stimulus levels. **(F)** Percentage of pulses that elicit action potentials as a function of stimulus level; lines connect data points from the same cell. Solid lines: Type A neurons; Dotted lines: Type B neurons. **(G)** Latency to peak of inward current for each elicited action potential as a function of amplitude; lines connect points from same cells. Solid and dotted lines: same as (F). Value = the mean ± S.E.

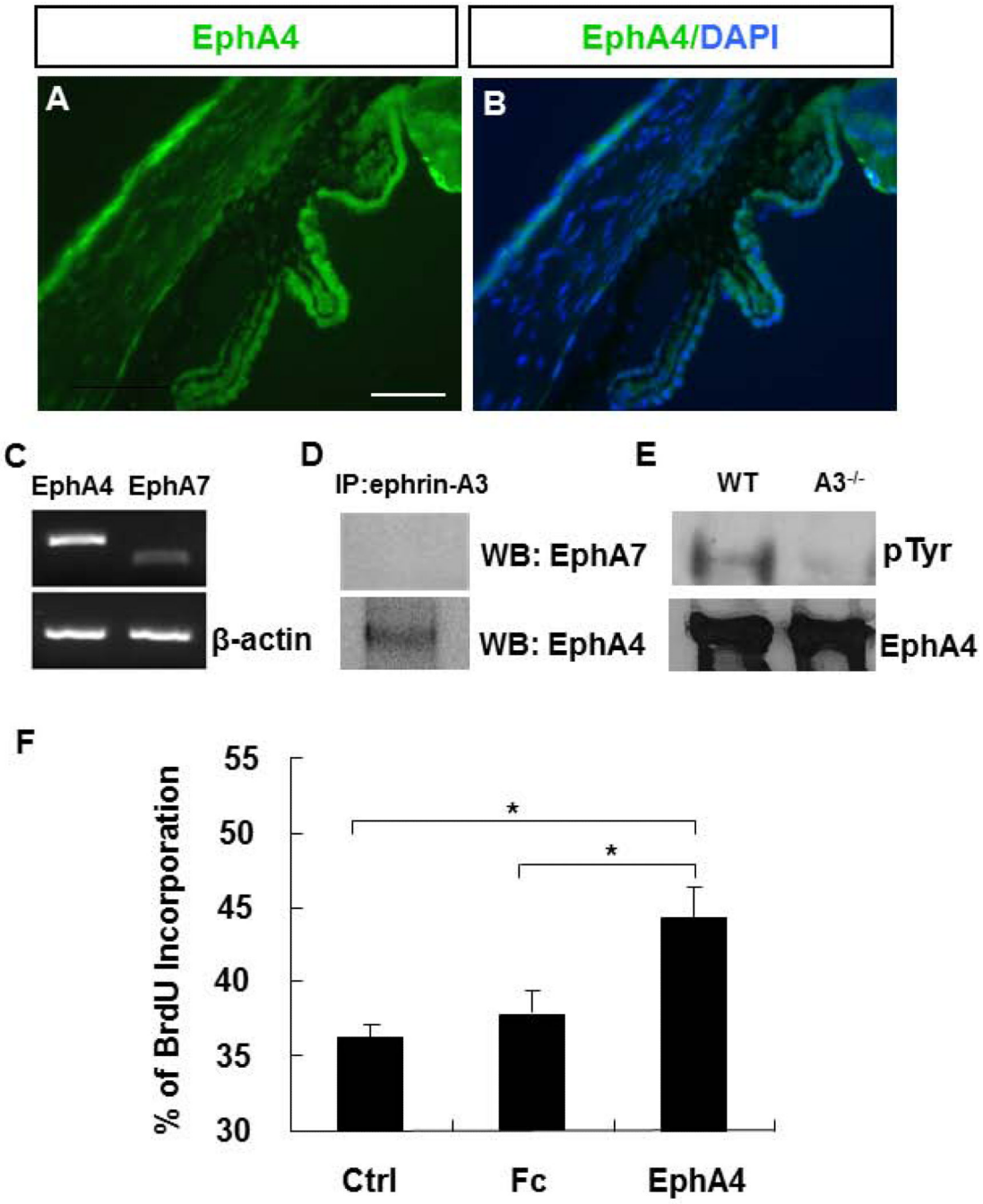

Figure 6.

Ephrin-A3 functioning through EphA4 in the adult CE. **(A,B**) Epifluorescence photomicrograph of a CE section (**A**) counterstained with DAPI (**B**) show EphA4 immunolabeling in the CE of adult wild-type mice. The CE section was counterstained with a nuclear marker DAPI to reveal the lamina structure **(B)**. Scale bar: 100 μm. **(C)** Results of semi-quantitative RT-PCR revealed a high level of EphA4 expression, but not EphA7, in CE-derived RSCs of adult wild-type mice; detection of β-actin mRNA levels was used as a loading control. **(D)** Immunoprecipitation of CE cell lysates of adult mice with ephrin-A3 antibody pulled down EphA4 instead of EphA7, further supporting the premise that ephrin-

A3 binds primarily to EphA4 in the adult CE. **(E)** Results of western blots show EphA4 phosphorylation in the CE cell lysates of wild-type, but not ephrin-A3$^{-/-}$ mice, suggesting that activation of EphA4 requires the presence of ephrin-A3. **(F)** Quantification of RSC proliferation was performed in dissociated NS cell cultures of wild-type mice that were untreated (Ctrl) or treated with control Fc (Fc) or soluble EphA4 (EphA4). Note that addition of soluble EphA4, but not control Fc, competed with the inhibitory effects of intrinsic EphA4 receptors on NS cells and significantly increased the percentage of BrdU incorporation or cell proliferation (*P<0.05 by One Way ANOVA).

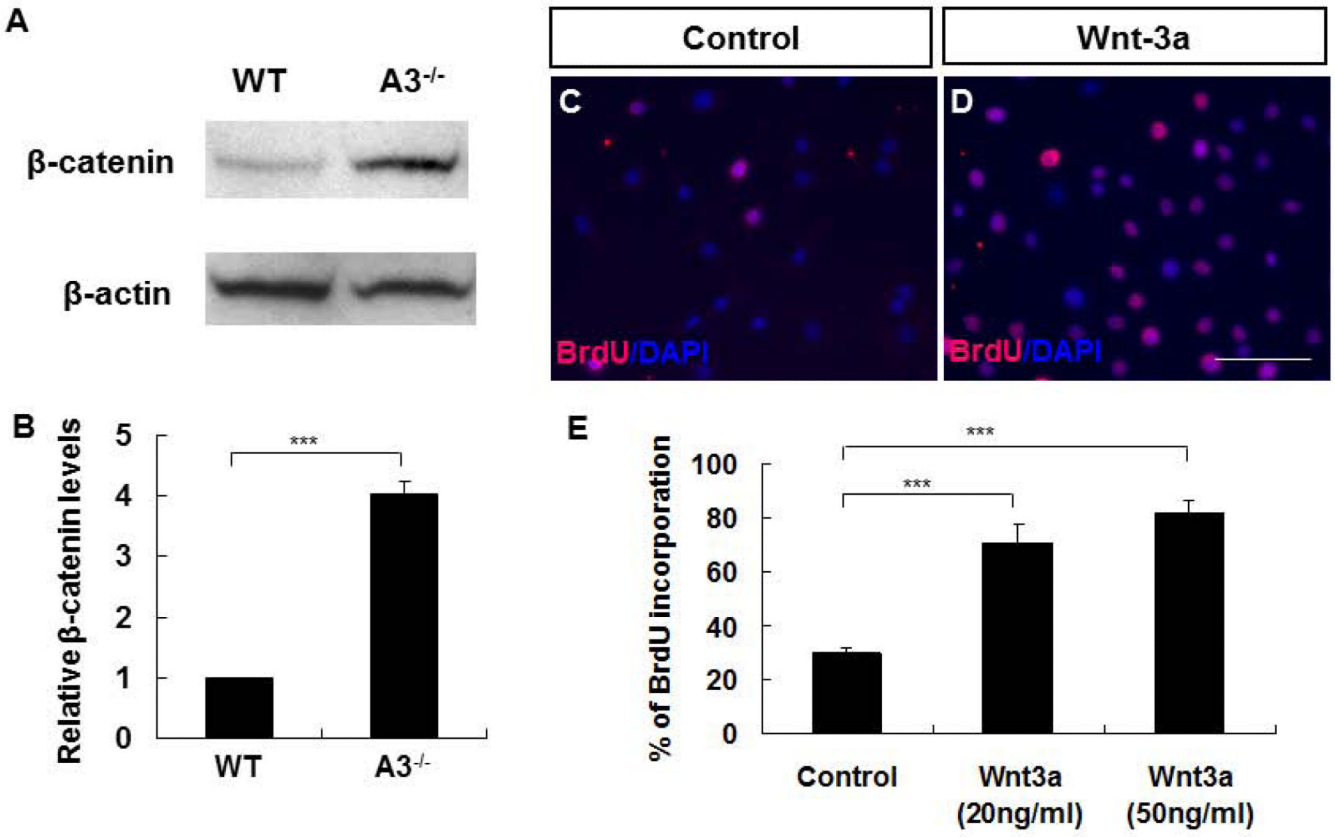

Figure 7.

Absence of ephrin-A3 increasing Wnt signaling to promote proliferation of CE-derived RSCs. **(A,B)** Representative western blots of triplicate experiments **(A)** and quantification of β-catenin expression **(B)** show an average of 4-fold increase in β-catenin levels in primary CE-derived NSs of ephrin-A3$^{-/-}$ mice, suggesting enhanced activity of the Wnt canonical pathway in their CE-derived cells than those of wild-type mice (**P<0.01 by two tailed student's t test). **(C-E)** Images represent BrdU incorporation assay **(C,D)** and quantification of BrdU incorporation **(E)** in dissociated CE-derived NS cell cultures of wild-type mice. Addition of Wnt3a alone was sufficient to promote cell proliferation and increase BrdU incorporation in cultures. Scale bar: 100 μm. (***P<0.001 by One Way ANOVA).